Electronic Supplementary Material (ESI) for Physical Chemistry Chemical Physics.

Electronic Supplementary Information for: Spectroscopy and Dynamics of Double Proton Transfer in Formic Acid Dimer

Kasper Mackeprang,[†] Zhen-Hao Xu,[‡] Zeina Maroun,[†] Markus Meuwly,[*,‡] and Henrik G. Kjaergaard[*,†]

Department of Chemistry, University of Copenhagen, Universitetsparken 5, DK-2100 Copenhagen Ø, Denmark, and Department of Chemistry, University of Basel, Klingelbergstrasse 80, 4056 Basel, Switzerland

E-mail: m.meuwly@unibas.ch; hgk@chem.ku.dk

Phone: +41(0)612673821; +45-35320334. Fax: +41(0)612673855; +45-35320322

[*]To whom correspondence should be addressed
[†]University of Copenhagen
[‡]University of Basel

Spectral Subtraction

The ratio between the partial pressure of dimer and monomer, $p_{\mathrm{dimer}}/p_{\mathrm{monomer}}$, becomes larger as the total pressure of formic acid (FA) and formic-*d* acid (*d*-FA) increases. As a result, an individual spectrum of the dimer can be obtained by subtraction of a scaled low-pressure spectrum from a high-pressure spectrum as follows:

$$S_{\mathrm{dimer}} = S_H - a \cdot S_L \tag{S1}$$

where S_{dimer} is the spectrum of the dimer, S_H is the high-pressure spectrum, S_L is the low-pressure spectrum and a is a scaling factor. The scaling factor is chosen such that monomer features are completely subtracted with a flat baseline to indicate a good subtraction. The pressures at which S_H and S_L were recorded as well as the a-values are summarized in Table S1.

Table S1: The pressures at which the low- and high-pressure spectra were recorded (p_L and p_H, respectively) in Torr and the scaling factors used (a)

	p_L	p_H	a
FA	0.46	11	3.9
d-FA	6.4	21	2.0

In Figure S1, the low- and high-pressure spectra of FA (left) and *d*-FA (right) are shown along with the residuals of the subtractions which are the dimer spectra. In the latter, the successful subtractions of the monomers are evident by comparison with the two upper panels. At 3570 cm^{-1}, where the OH-stretching band of the monomer is seen in the original spectra, there is now a flat baseline. It can also be seen by the flat baseline in the previous positions of several other bands (e.g. the C-O-H bend at 641 cm^{-1}, C-O(H) stretch at 1105 cm^{-1}, and the C=O stretch at 1777 cm^{-1} of FAM and the O-C=O bend at 629 cm^{-1}, D-C-O bend at 970 cm^{-1}, C-O(H) stretch at 1143 cm^{-1}, and the C=O stretch at 1760 cm^{-1} of *d*-FAM). In the performance of these spectral subtractions, it should be kept in mind

that for the spectra to be used for a quantitative purpose, the low-pressure spectrum should be recorded at such a low vapor pressure that the dimer formation is negligible. This is important so as not to reduce the signal of the dimer from the high-pressure spectrum in the subtraction. The disadvantage of using the spectra recorded at extremely low pressure, however, is a low signal to noise ratio. As our focus in this study is purely qualitative, we have chosen to record the low-pressure spectra at more elevated pressures where both monomer and dimer are present, but where the signal to noise ratio is much higher.

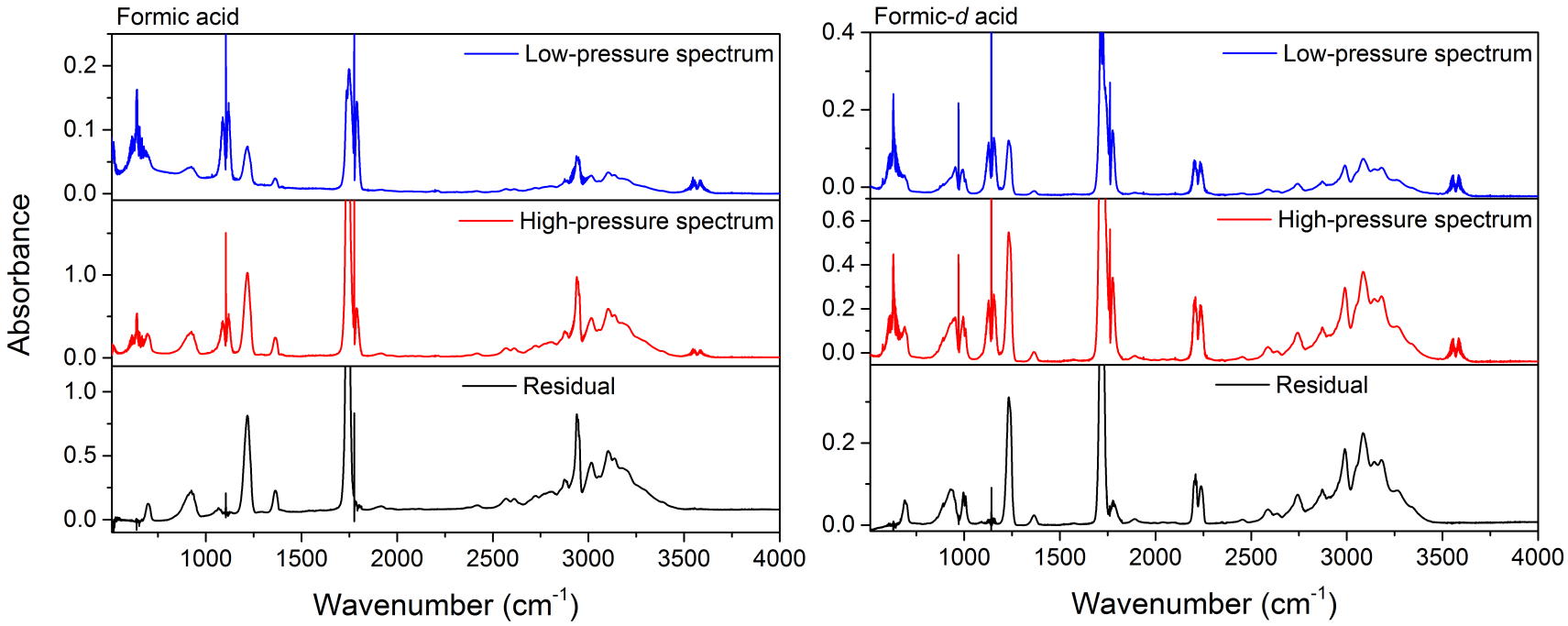

Figure S1: The low-pressure (upper panel) and high-pressure (middle panel) spectra used for the spectral subtractions to obtain the spectra of the dimers (lower panel) of FAD (left) and *d*-FAD (right)

Computational Details

Table S2: Parameters for MMPT-MP2 and MMPT-B3LYP PESs. See reference **?** for details of the implementation.

		MMPT-B3LYP		MMPT-MP2	
Parameters		V_{SDM}	V_{SSM}	V_{SDM}	V_{SSM}
p_1	kcal/mol	1338938	1338863	1339070	1338978
p_2	Å^{-1}	0.707	1.331	0.920	1.292
p_3	Å	-10.603	-5.251	-7.061	-4.872
p_4	kcal/mol	-1338591	-1338667	-1338459	-1338551
p_5	Å^{-1}	0.537	-0.792	0.685	-0.645
p_6	Å^{-2}	0.808	1.134	0.753	1.076
p_7	Å	76.535	54.564	73.937	42.080
p_8	Å^{-1}	2.777	2.602	2.817	2.516
p_9	Å	0.079	0.104	0.076	0.090
p_{10}	kcal/(mol$\cdot$ deg^2)	0.002	0.002	0.002	0.002
p_{11}	kcal/mol	32.85	62.78	51.03	113.38

The functional form of V_{SDM} and V_{SSM} is $V(R,\rho,\theta) = V_0(R,\rho) + k\theta^2$ in which[?]

$$V_0(R,\rho) = D_{eq}(R)[1 - e^{-\beta(R)(\rho-\rho_{eq}(R))}]^2 + D_{eq}(R)[1 - e^{-\beta(R)(1-\rho-\rho_{eq}(R))}]^2 - D_{eq}(R) - c \quad \text{(S2)}$$

Each of the coefficients is fitted to the following parametrizations;

$$\begin{aligned} D_{eq}(R) &= p_1[1 - e^{-p_2(R-p_3)}]^2 \\ \beta(R) &= p_5 + p_6 R \\ \rho_{eq}(R) &= p_7 e^{-p_8 R} + p_9 \\ p_{10} &= k,\ p_{11} = c \end{aligned} \quad \text{(S3)}$$

Figures

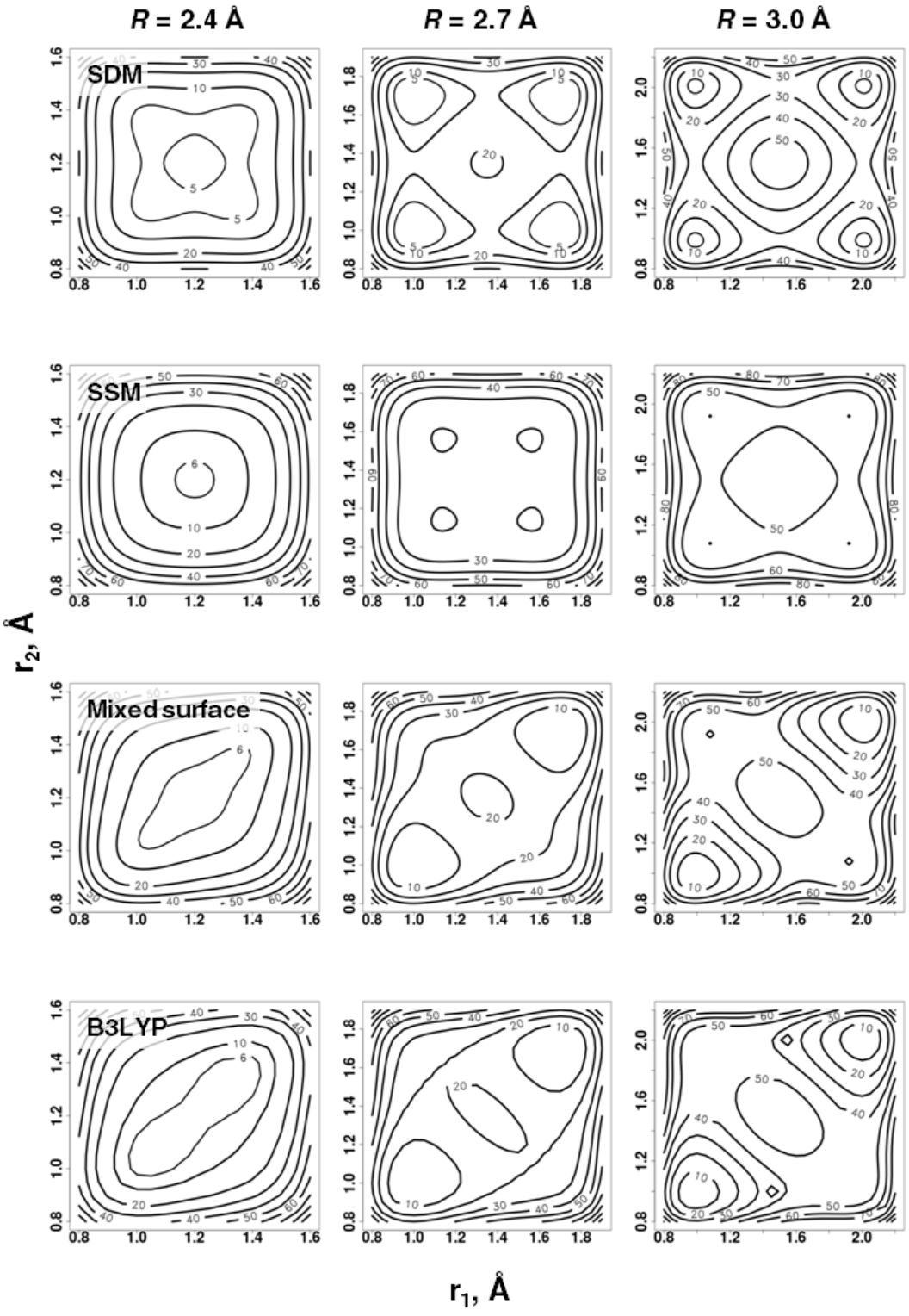

Figure S2: 2D potential energy surfaces for different values of the D–A separation, R ($R \in [2.4\ \text{Å}, 2.7\ \text{Å}, 3.0\ \text{Å}]$). From top to bottom: the SDM PES, the SSM PES, the mixed MMPT PES and the *ab initio* B3LYP/6-31G(d,p) PES to which the mixed PES was fitted. The energies listed on the contour lines are in kcal mol^{-1}

Table S3: The fixed point charges for carbons (C), oxygens (O), hydrogens (H), and the transferring hydrogens (H_T) from an NBO analysis at the B3LYP/6-31G(d,p) TS structure for computing the dipole moment

Atom	Charge (e)
C	0.63
O	-0.675
H	0.2
H_T	0.52

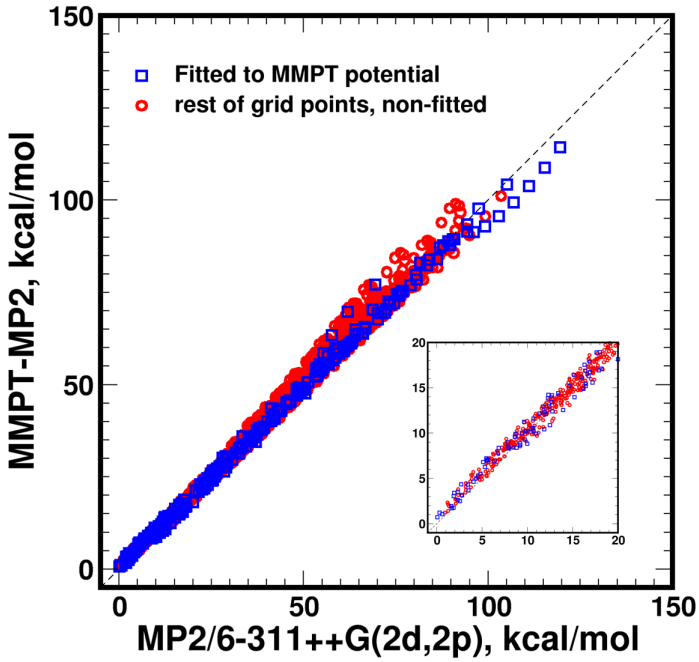

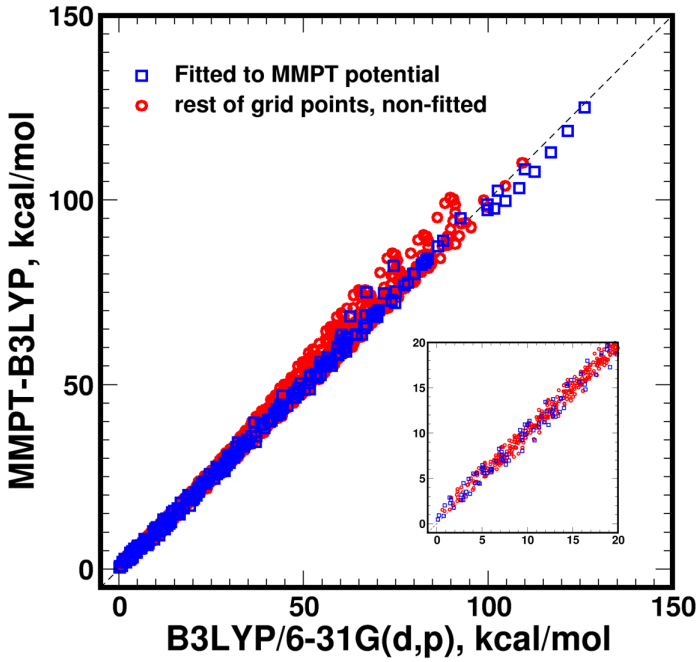

Figure S3: Correlation of potential energy between MMPT, MP2, and B3LYP levels

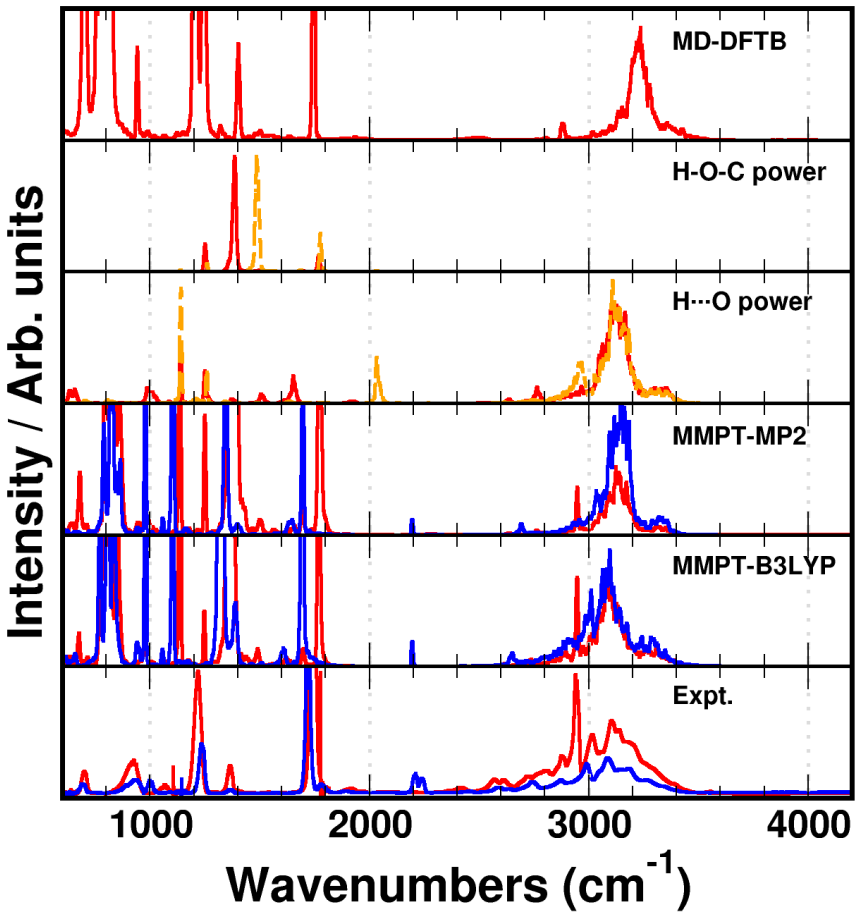

Figure S4: Simulated spectra of FAD (red) and *d*-FAD (blue) obtained from MD simulations (second and third panel from bottom). For the simulations with the MMPT force field the barrier heights were morphed to 5.1 kcal mol^{-1} and 7.2 kcal mol^{-1} for MMPT-B3LYP and MMPT-MP2, respectively. The HOC- and H$\cdots$O (H-bond) power spectra from simulations (*d*-FAD) with MMPT-MP2 and two values of the H-bending force constant $k = 17.5$ kcal mol^{-1} (red) rad^{-2} and $k = 33$ kcal mol^{-1} rad^{-2} (dashed orange) are given in the second and third panel from the top. Note the strong coupling between the H$\cdots$O power spectrum and other modes. The experimental spectra of FAD and *d*-FAD have been included for comparison.

References

() Lammers, S.; Lutz, S.; Meuwly, M. Reactive force fields for proton transfer dynamics. *J. Comput. Chem* **2008**, *29*, 1048–1063.